POLİTEKNİK DERGİSİ

JOURNAL of POLYTECHNIC

ISSN: 1302-0900 (PRINT), ISSN: 2147-9429 (ONLINE)
URL: http://dergipark.org.tr/politeknik

Confirmation of johnson-cook model parameters for nimonic 80A alloy by finite element method

Nimonic 80A alaşımının johnson-cook model parametrelerinin sonlu elemanlar yöntemiyle doğrulanması

***Yazar(lar) (Author(s))**: Mehmet Erdi KORKMAZ[1], Mustafa GÜNAY[2]*

ORCID[1]: 0000-0002-0481-6002

ORCID[2]: 0000-0002-1281-1359

Bu makaleye şu şekilde atıfta bulunabilirsiniz(To cite to this article): Korkmaz, M.E and Günay, M., "Confirmation of johnson-cook model parameters for nimonic 80A alloy by finite element method", ***Politeknik Dergisi***, 23(3): 625-632, (2020).

Erişim linki (To link to this article): http://dergipark.org.tr/politeknik/archive

DOI: **10.2339/politeknik.555271**

Confirmation of Johnson-Cook Model Parameters for Nimonic 80A alloy by Finite Element Method

Highlights

- *The determination of material constitutive model (Johnson-Cook) of Nimonic 80A superalloy.*
- *Three different types of compression tests (quasi-static, dynamic and high temperatures) in order to determine the equation parameters.*
- *The confirmation of Johnson-Cook parameters of Nimonic 80A superalloy.*
- *A suggestion of finite element simulation of any plastic deformation processes such as forging, rolling and deep drawing by using JC parameters of Nimonic 80A material as a next study.*

Graphical Abstract

The aim of the study is to confirm the predetermined J-C model parameters for Nimonic 80A superalloys using finite element method.

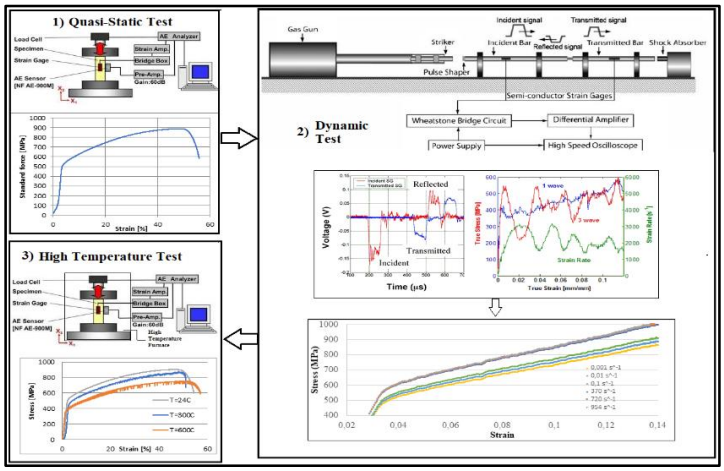

Figure. Experimental procedure

Aim

The aim of the study is to confirm the predetermined J-C model parameters for Nimonic 80A superalloys using finite element method.

Design & Methodology

JC parameters of Nimonic 80A nickel-based superalloys were identified via quasi-static tests, dynamic tests and different temperature tests.

Originality

By considering the literature, it is obviously seen that there is no study on simulation of plastic deformation processes based on finite element method for Nimonic 80A superalloy.

Findings

The mean deviation between experimental results and simulation results obtained with FEM were calculated as average of %3.23.

Conclusion

Consequently, the Johnson-Cook model parameters of Nimonic 80A was confirmed based on overall results. Hence, it was concluded that JC model parameters of the material can be confidently used for any plastic deformation processes.

Declaration of Ethical Standards

The author(s) of this article declare that the materials and methods used in this study do not require ethical committee permission and/or legal-special permission.

Confirmation of Johnson-Cook Model Parameters for Nimonic 80A alloy by Finite Element Method

Araştırma Makalesi / Research Article

Mehmet Erdi KORKMAZ*, Mustafa GÜNAY

Department of Mechanical Engineering, Faculty of Engineering, Karabük University, Karabük, Turkey

(Geliş/Received : 17.04.2019 ; Kabul/Accepted : 08.06.2019)

ABSTRACT

Nimonic 80A superalloy is frequently used due to its high creep resistance, oxidation resistance and high resistance to high temperature corrosion. On the other hand, due to compatibility of simulation of plastic deformation processes, Johnson-Cook model is chosen among the materials models such as Zerille Armstrong, Bordner Partom, Steinberg-Guinan etc. In this study, primarily, quasi-static compression tests were performed for 10-3, 10-2 and 10-1 s-1 strain rates at room temperature. Secondly, dynamic compression tests were secondly conducted at high strain rates ranging from 370 to 954 s-1 using the Split Hopkinson Pressure Bar (SHPB) apparatus. Then, the compression tests were conducted at a temperature level from 24~200 °C at the reference strain rate. Johnson-Cook model parameters of Nimonic 80A were determined by analyzing the data obtained from the tests. Lastly, the compression simulations with finite element method (FEM) were performed in ANSYS Workbench to confirm the accuracy of the parameters. In the light of the results, it was determined that there is an average of %3.23 deviation between the experimental and the simulation values. The result showed that accuracy of the Johnson-Cook parameters for Nimonic 80A superalloy was verified with FEM.

Keywords: Nimonic 80A, johnson-cook parameters, finite element method, split-hopkinson pressure bar.

Nimonic 80A Alaşımının Johnson-Cook Model Parametrelerinin Sonlu Elemanlar Yöntemiyle Doğrulanması

ÖZ

Nimonic 80A alaşımı, yüksek sürünme mukavemeti, oksidasyon direnci ve yüksek sıcaklıktaki korozyona karşı güçlü direnci nedeniyle tercih edilmektedir. Bu makale Nimonic 80A süperalaşımının malzeme yapısal denklemini (Johnson-Cook parameters) belirlemek için yazılmıştır. Literatürdeki farklı malzeme yapısal denklemlerinin (Zerille Armstrong, Bodner Partom, Johnson-Cook) arasından Johnson-Cook modeli tercih edilmiştir. Denklem parametrelerinin belirlenmesi için 3 farklı tipte basma testleri uygulanmıştır. Bunların ilki oda sıcaklığında gerçekleşen yarı-statik basma testleridir. Bu testler 10-3, 10-2 ve 10-1 s-1 gerinim hızlarında gerçekleştirilmiştir. Dolayısıyla bütün testler için referans gerinim hızı 10-3 seçilmiştir. İkinci test olarak oda sıcaklığında Split -Hopkinson çekme cihazı kullanılarak yüksek gerinim hızlarında (370 ~ 954 s-1) basma testleri gerçekleşmiştir. Son olarak referans gerinim hızında (10^-3 s^-1) yüksek sıcaklıklarda (24 ~ 200 °C) basma testleri yapılmıştır. Testlerin birbiri ile uygun olduğu gözlemlenmiş olup, bu testlerden elde edilen veriler ile malzemeye ait Johnson-Cook parametreleri belirlenmiştir. Son olarak, sonlu elemanlar yöntemi vasıtasıyla gerçekleştirilen basma testi simülasyonları parametrelerin uygunluğunu onaylamak adına ANSYS Workbench yazılımında yapılmıştır. Bu sonuçlar ışığında, deneysel ve simülasyon sonuçları arasında %3.23 sapma elde edilmiştir. Bu sapma miktarı, Nimonic 80A alaşımına ait belirlenen Johnson-Cook model parametrelerinin doğruluğunu kanıtlamaktadır..

Anahtar Kelimeler: Nimonic 80A, johnson-cook parametreleri, sonlu elemanlar yöntemi, split-hopkinson basma cihazı.

1. INTRODUCTION

The Nimonic 80 A superalloys are incidents to nickel-based superalloys and is suitable for manufacturing of machine parts working at high temperature. It is chemically a complex superalloy whose main components of the alloying elements are Cr, Mo, W, Ti, Ta, Al. Nimonic 80A alloys are commonly used in jet engine, gas turbine because of their high creep strength, oxidation resistance and strong resistance to high temperature corrosion [1–3].

It is known that some materials have higher hardness as they deform plastically. This condition, called strain hardening, results in an increase in the number of dislocations in the material depending on the amount of deformation. The strain hardening coefficient indicated by "n" is used to express how a material get strong due to its deformation. Being higher of this coefficient means that the material has a high strain hardening capacity and therefore is ductile. Unlike this, some materials appear to strain-rate hardening depending on the rate of

**Sorumlu Yazar (Corresponding Author)*
e-posta : merdikorkmaz@karabuk.edu.tr

deformation. This means that when two tensile tests at different speeds are applied to a material with this property, the different stress-strain curves are obtained. In contrast, the curve of the sample for high speed tensile test is shifted upward compared to the other and it is understood that the material is strengthened. Especially, due to the fact that the investigations on plastic deformation processes are exclusive and time wasting, finite element (FE) modelling of the plastic deformation processes is practical as an alternate solution method [4–6]. Thus, the deformation behavior of materials can be analyzed in deformation processes and it is probable to make an important contribution to decrease the experimental costs. In this regard, the FE models have become a crucial tool in investigations of plastic deformation processes and analysis of engineering designs.

Depending upon the finite element method, the experimental results (stress, surface quality, etc.) of manufacturing process [7–11] need to be well-suited with the simulational results found from the computers' software. In this regard, that is very significant in order to model the material properly in simulation package. Several constitutive materials models are planned representing high strain behaviours at extensive ranges of strain rate and temperature [12]. The models are Zerille-Armstrong, JC model, modified JC model and it is underlined that the JC model is frequently used for various softwares performing FE analysis [13]. In order to determine the J-C material model, it is essential to conduct dynamic experiments along with quasi-static and high temperature experiments. That needs a SHPB test setup, which is immensely studied [14–18]. Many studies pertain to the identification of the J-C model parameters were performed via the setups. With this regard, Karkalos et al. optimized the J-C model parameters for AISI 316L stainless steel using high strain rate range and temperature ranges [19]. Tan et al. determined the JC model parameters of Inconel 718 via compression tests [20]. Limbadri et al. determined the J-C material parameters of the Zircaloy-4 and investigated the stress variations for rolled sheet [21]. Ducobu et al. optimized the predetermined 20 J-C model parameters for Ti6Al4V alloy and determined the best JC model for orthogonal cutting process [22]. By considering the literature, it is obviously seen that there is no study on simulation of plastic deformation processes based on finite element method for Nimonic 80A superalloy although the material is important in aerospace areas requiring high temperature characteristics. In this case, the aim of the study is to confirm the predetermined J-C model parameters for Nimonic 80A superalloys [23] using finite element method.

2. MATERIAL and METHOD

2.1 Material and Equipment

The mechanical and physical properties and chemical composition of Nimonic 80A alloys were given in Tables 1 and 2, respectively [23].

Experiments performed to identify the JC material parameters for Nimonic 80A alloys consist of 3 steps. Firstly, dynamic experiments at high speeds such as 370-954 s-1 were performed. The compression sample used for this step is shown in Fig. 1b before and after the test. Dynamic experiments were carried out on SHPB pertaining to the Material Laboratory of Ghent University (Fig. 1a). Figure 1b shows the compression test samples used also for the quasi-static and high-temperature experiments carried out with the Zwick / Roell Z600 Universal Testing Machine, which is located at the Iron and Steel Institute of Karabük University. Figure 2 shows the experimental procedure for all the steps.

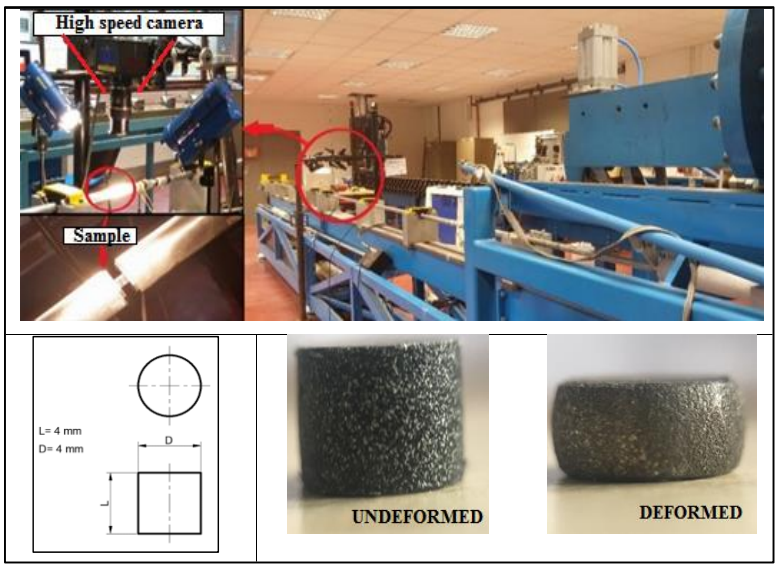

Figure 1. a) Split Hopkinson Pressure Bar, b) the compression sample

Table 1. Mechanical and physical specifications of Nimonic 80 A

Material	*E (GPa)*	*T_m (°C)*	*α (10^{-6}/°C)*	*k (W/m°C)*	*υ*	*ρ (kg/m^3)*	*c_p (J/kg°C)*
Nimonic 80A	183	1365	12.7	11.2	0.3	8190	448

Table 2. Chemical composition of Nimonic 80 A, % weight

C	*Si*	*Mn*	*P*	*Al*	*S*	*Co*	*Fe*	*Ti*	*Cr*	*Ni*
0.052	0.06	0.02	0.005	1.35	0.001	0.05	0.8	2.43	19.2	Balance

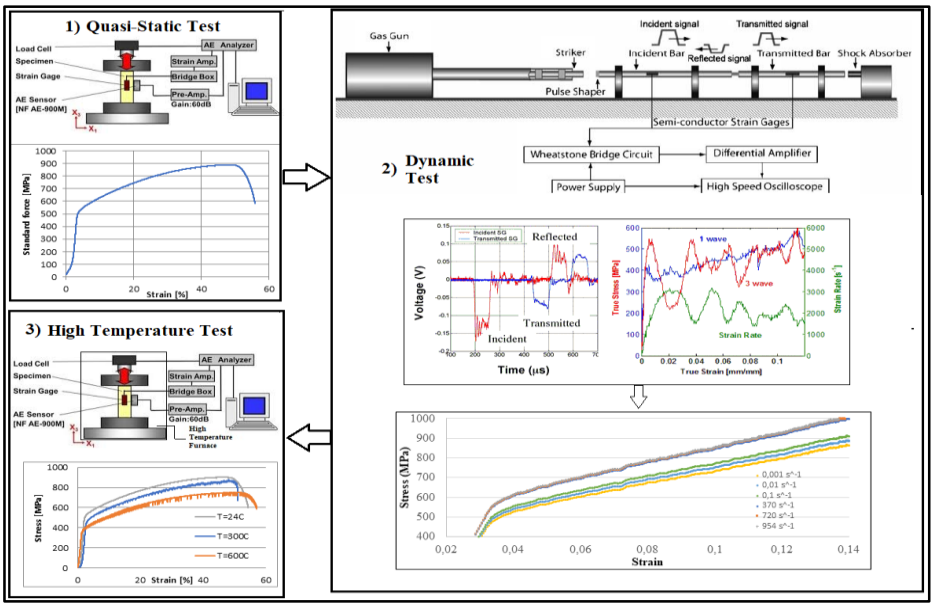

Figure 2. Experimental procedure

2.2 Determination of Johnson-Cook Parameters

The plastic deformation behaviour of the Nimonic 80A alloys is taken into consideration by J-C model. The material model is mainly appropriate to model the higher deformation rate of engineering materials. They are frequently applied for adiabatic transient dynamic analyzes. In J-C models, it is supposed that the yield stress (σ^0) is:

$$\sigma^0 = (A + B(\varepsilon^p)^n)\left(1 + C\, ln\left(\frac{\dot{\varepsilon}^p}{\dot{\varepsilon}_0}\right)\right)\left(1 - \left(\frac{T - T_r}{T_m - T_r}\right)^m\right) \quad (1)$$

Here parameters found from mechanical experiments that are A, B, C, n and m are yield strength under room temperature, strain hardening, strain rate constant, strain hardening constant and thermal softening constant, respectively. The additional parameters ε^p, $\dot{\varepsilon}^p$, $\dot{\varepsilon}_0$, T_r, T_m and T are equivalent plastic strain, plastic strain rate, reference strain rate, room temperature, melting temperature and reference temperature, respectively. Also, $\dot{\varepsilon}_0$ and C are usually measured at or below the reference temperature.

2.3 Confirmation of Johnson-Cook Parameters

Finite element method (FEM) was applied with same deformation conditions since the results obtained from experimental studies should be approved with numerical modeling. Explicit Dynamic module of ANSYS Workbench was used for finite element analysis. Firstly, the Johnson-Cook material parameters determined with experiments were adapted to the software material data. Afterwards, the compression test simulations were performed according to the same compression test conditions with different strain rates (10^{-3}, 10^{-2}, 10^{-1}, 370, 720 and 954 s^{-1}). Finally, the experimental and FEM results were compared to confirm the J-C model parameters identified for Nimonic 80A alloys.

3 RESULTS AND DISCUSSION

3.1 Identification of *A, B and n* Parameters

In J-C material models, ***A*** specifies the yield strength at the reference strain rates (0.001 s^{-1}). Figure 3 shows that ***A*** parameter (strain at 24 °C and 0.001 s^{-1}) was measured as 487 MPa the data acquisition software of compression test setup according to the experiment performed at 10^{-3} s^{-1}.

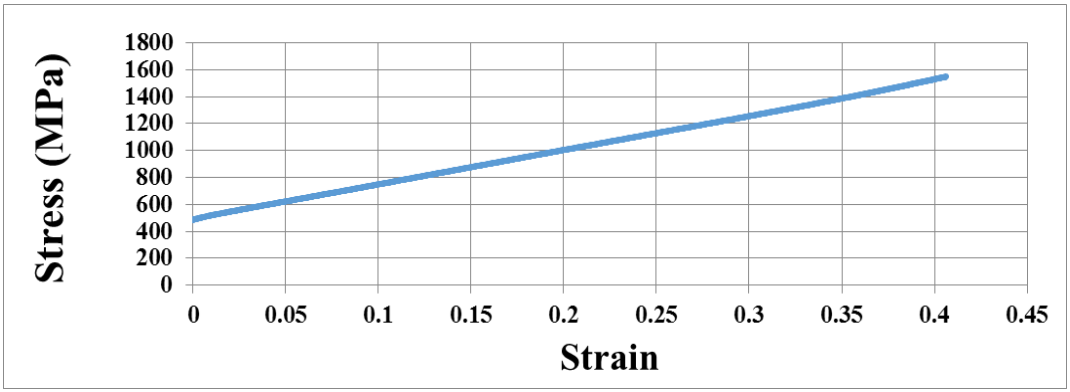

Figure 3. The stress-strain diagram in reference strain rate and room temperature

According to the test at 10^{-3} s^{-1}, the point which the yield strength starts is supposed as zero strain, and the constant of ***B*** and ***n*** are identified consistent with the increase in strength value at each amounts of deformation. This statement is between the yield stresses and ultimate stresses. Based on Figure 3, compressive stresses at 0.10, 0.20 and 0.30 strains were found to be about 748, 1003 and 1254 MPa. According to these average stress strain values and Equation 2, the constants ***B*** and ***n*** are calculated as 2511 MPa and 0.983, respectively.

$$\sigma^0 = (A + B(\varepsilon^p)^n) \quad (2)$$

3.2 Identification of *C* Parameter (*C* Parametresinin Belirlenmesi)

In JC material models, ***C*** parameter indicate the strain rate constant. It was beheld that the compressive strength values increase with the increases of strain rates in the compression experiments performed at the room temperatures. That is reliable with the study in the literature [13]. In Fig. 4, the variations in stress values are shown by increasing the strain rate. Moreover, the strain and the displacement values at strain rate of 954 s^{-1} were approved with digital image correlation (DIC) by high speed camera (Fig. 1a) and the DIC images were given in Fig. 4.

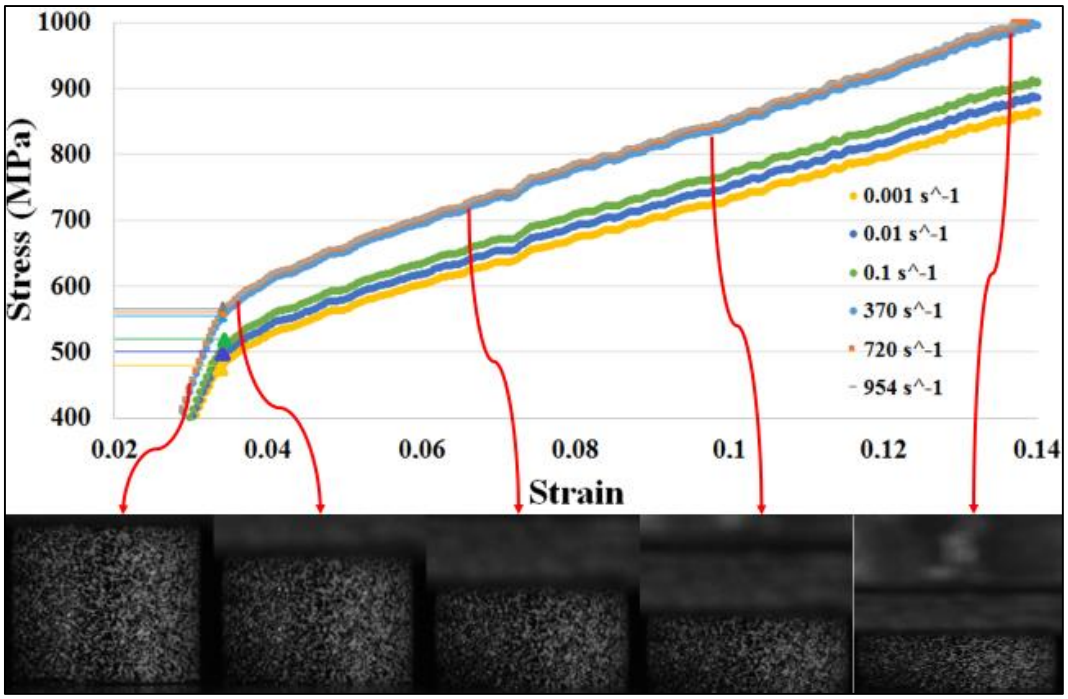

Figure 4. Stress-strain diagram in different strain rates

According to Fig. 4, it was measured from the data acquisition system that the yield stresses were 487, 500 and 513 MPa from the data acquisition software of compression test setup at 0.001, 0.01 and 0.1 s^{-1} strain rate values. At dynamic strain rate values (400, 700 and 1000 s^{-1}), yield strength increased to 562, 566 and 568 MPa, respectively, in the predictable range. The C constant is calculated as 0.0122 based on Eqn.3 and Fig.5 obtained from average stress-strain curves in different strain rates.

$$\sigma = \sigma^0 \left(1 + C\ ln\left(\frac{\dot{\varepsilon}^p}{\dot{\varepsilon}_0}\right)\right) \quad (3)$$

3.3 Identification of *m* Parameter

The parameter of ***m*** indicates the temperature in the Johnson-Cook material model. In the compression test performed at 10^{-3} s^{-1}, the yield stress values commonly reduced with increasing test temperatures, as stated in some studies [3,24,25]. The variation in the compression stress by increase in the test temperatures is given in Figure 5.

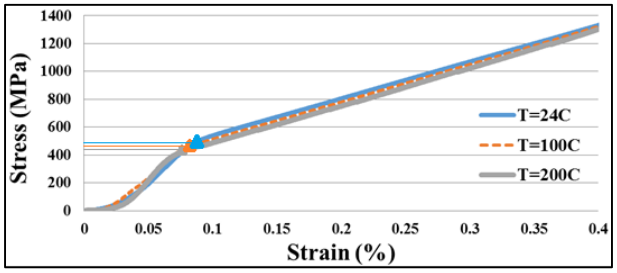

Figure 5. Stress-strain diagram in different temperatures

The yield stress was measured as 487, 465 and 450 MPa from the data acquisition software of compression test setup for 24, 100 and 200 °C, respectively. Then, Figure 5 was created by the experimental data from different temperature tests. The constant of ***m*** was calculated as 1.162 by using Eqn. 4 based on the stress-strain diagram.

$$\sigma = \sigma^0 \left(1 - \left(\frac{T - T_r}{T_m - T_r}\right)^m\right) \quad (4)$$

The Johnson-Cook model parameters of the Nimonic 80 A super alloy were determined by considering the quasi-static, dynamic and different temperature test. The values of overall parameters were given in Table 3.

Table 3. JC parameters of Nimonic 80A [23].

A (MPa)	*B (MPa)*	*n*	*C*	*m*	$\dot{\varepsilon}_0$ (s^{-1})
487	2511	0.983	0.0116	1.162	10^{-3}

3.4. Finite Element Modelling Results

Since the results from experimental studies should be approved with numerical modeling, finite element modeling was performed with same deformation conditions. ANSYS Workbench (Explicit Dynamic module) was used by adapting JC material parameters to the software material data [26-29]. After this step, the compression test simulations were performed according to same compression test conditions (experimental) with different strain rates (10^{-3},10^{-2},10^{-1}, 370, 720 and 954 s^{-1}).

In engineering analysis based on finite element method, the mesh structure and mesh size are very important issue in terms of consistency between the simulation and experimental results. 3D and 10-node tetrahedral mesh structure was preferred due to cylindrical shape of the specimen (Fig. 6). Mesh size was determined as mesh-dependency method. For the first simulation (954 s^{-1}), the results were 620, 600, 588 and 585 MPa with the mesh size of 1, 0.5, 0.2 and 0.1 mm, respectively (Table 4). The mesh size of 0.1 mm was determined as actual mesh size due to less change of stress values after the transition of 0.2 to 0.1 mm. Thus, the mesh size less than 0.1 mm was not preferred because less mesh size means much solving time.

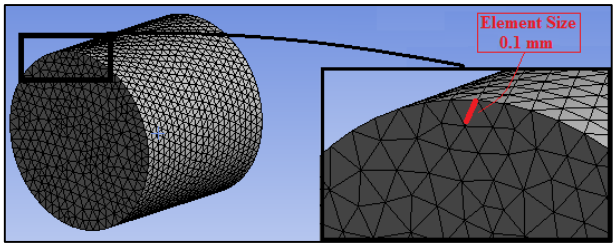

Figure 6. The element size of the mesh structure

Table 4. Mesh-dependency method

Element size (mm)	Yield stress (σ, MPa)
1	620
0.5	600
0.2	588
0.1	**585**

Figure 7 shows the yield stresses for experimental and numerical analysis in 10^3 s^{-1} strain rates. The actual value is 568 MPa when the simulated value is 585 MPa, and so the deviation between actual and modeling result were calculated as %2.98.

The yield stresses obtained with experimental and FEM at 370 s^{-1} strain rate was displayed in Figure 8. The simulated yield stress was calculated as 579.68 MPa, when the experimental value was found as 562 MPa, and so the deviation was calculated as %3.15.

According to Figure 9, the simulated yield stress was calculated as 531.26 MPa at 10^{-1} s^{-1} strain rate, when the experimental value was found 513 MPa, and so the deviation was calculated as %3.56.

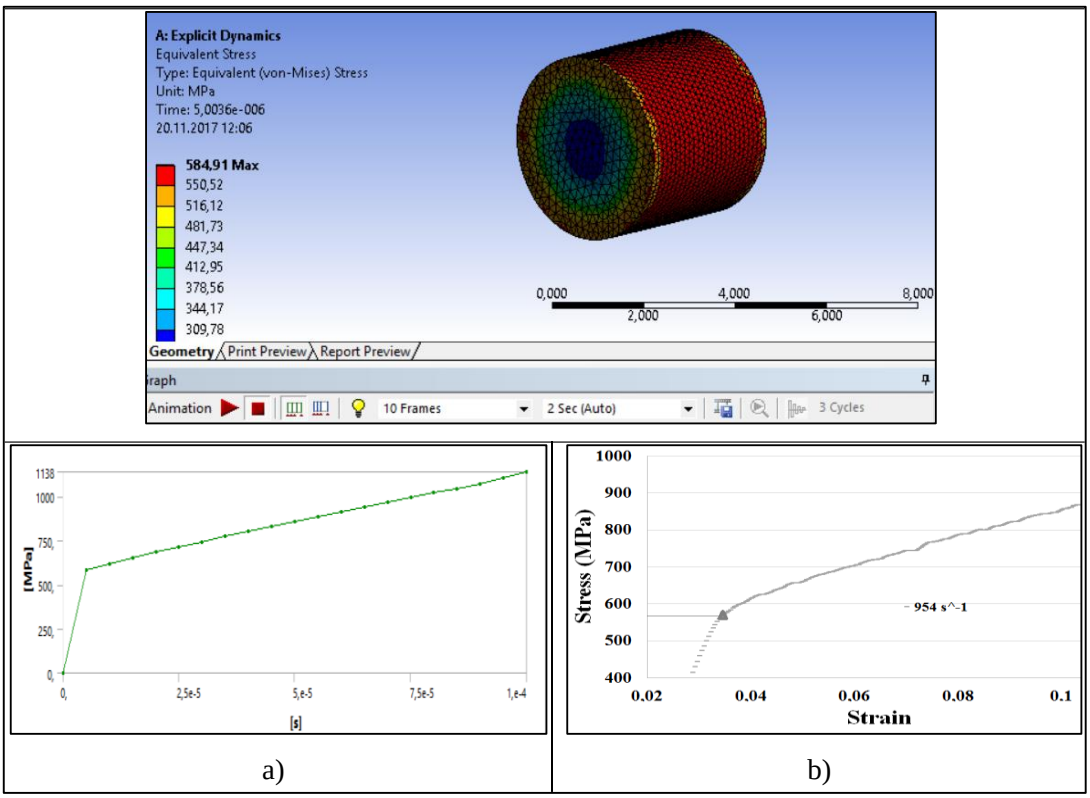

Figure 7. Stress-strain graph at 954 s^{-1} strain rate, a) Simulation, b) Experimental

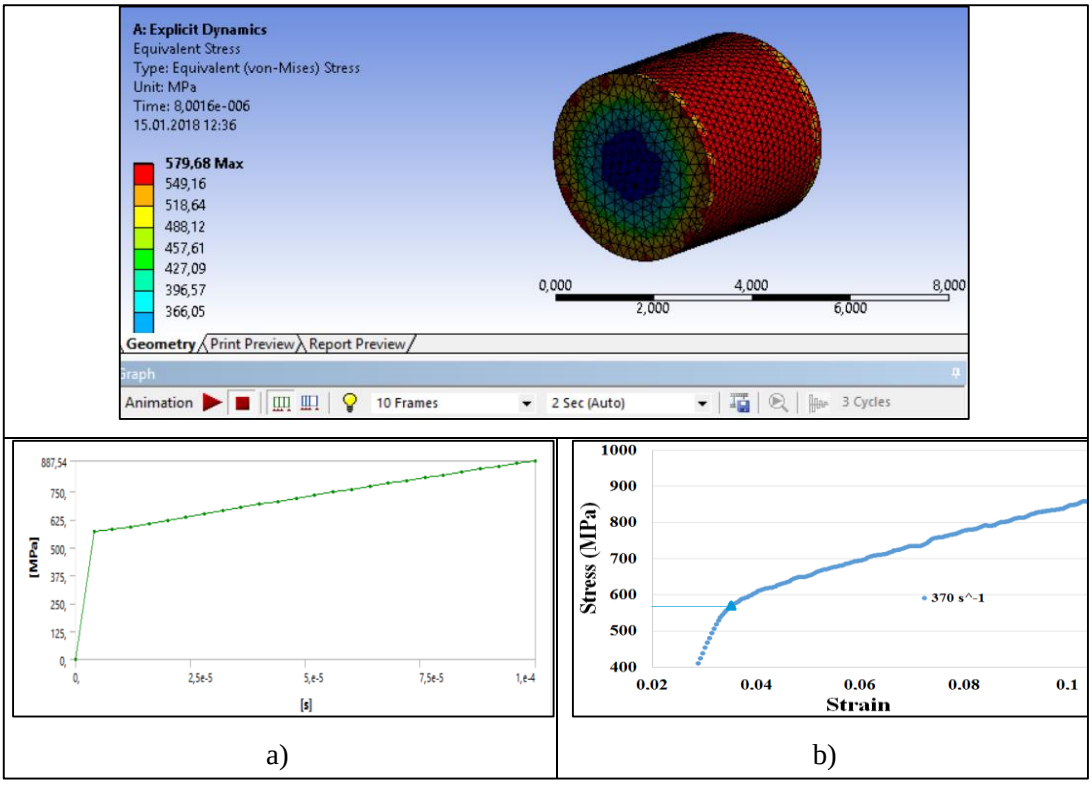

Figure 8. Stress-strain graph at 370 s^{-1} strain rate, a) Simulation , b) Experimental

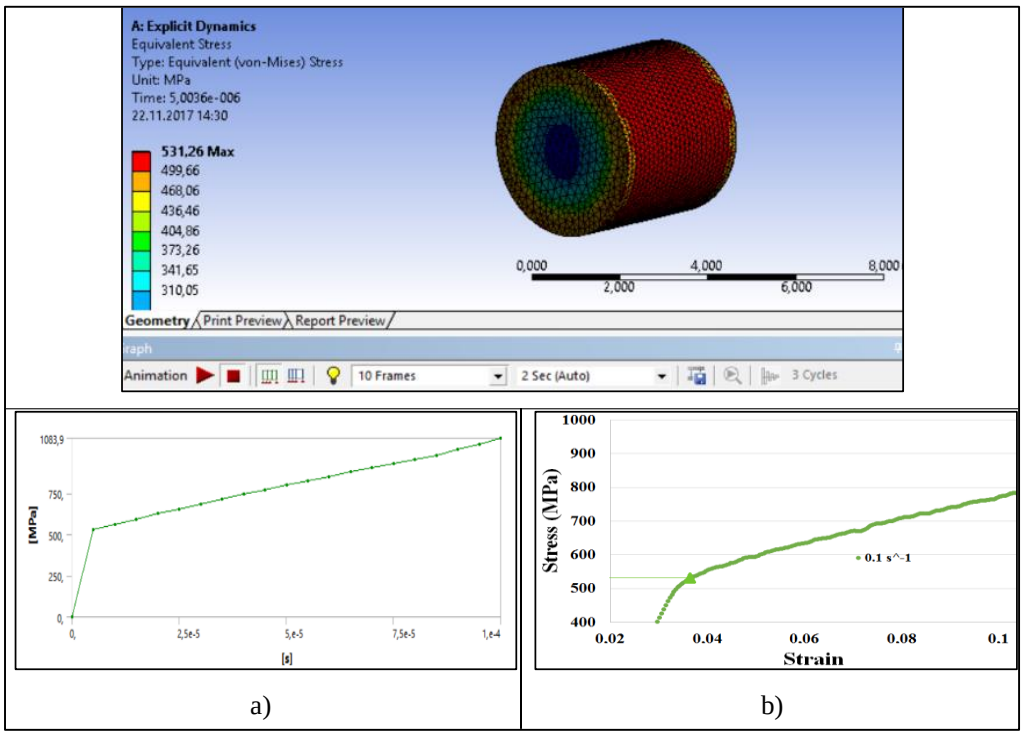

Figure 9. Stress-strain graph at 10^{-1} s^{-1} strain rate, a) Simulation, b) Experimental

Table 5. The deviations between simulation and experiment results

Strain rate (s^{-1})	Experimental results (σ, MPa)	Simulation results (σ, MPa)	Deviation (%)
0.001	487	502.83	3.25
0.01	500	516.60	3.32
0.1	513	531.26	3.56
370	562	579.68	3.15
720	566	583.66	3.12
954	568	584.91	2.98
		Mean deviation	**3.23**

The mean deviation between experimental results and simulation results obtained with FEM were calculated as average of %3.23. Consequently, the Johnson-Cook model parameters of Nimonic 80A was confirmed based on overall results. Hence, it was concluded that JC model parameters of the material can be confidently used for any plastic deformation processes.

4. CONCLUSION

In the finite element analysis software, the material structural equation of workpiece material (Zerill Armstrong, Bodner Partom, Johnson-Cook) must be found in order to simulate plastic deformation processes such as machining, deep drawing, bending and forging, etc. Generally, the analysis of the finite elements for any plastic deformation process has usually used the default material equation parameters. Our goal is to confirm the JC parameters of a new material used in aerospace technology in the future. For this reason, in this study, JC parameters of Nimonic 80A nickel-based superalloys were identified via quasi-static tests at low speeds (10-3-10-1 s-1), dynamic tests at high speeds (370-954 s-1) and different temperature tests (24-200 °C). By using the identified JC parameters of Nimonic 80A materials, a finite element analysis of the compression tests was performed with same experimental conditions in the next step. The mean deviation between experimental results and simulation results obtained with FEM were calculated as average of %3.23. Consequently, the Johnson-Cook model parameters of Nimonic 80A was confirmed based on overall results. To conclude, a FE modeling of other plastic deformation processes (bending, deep drawing, crash test, etc.) generated compressive load can be performed with the JC parameters as a next study.

ACKNOWLEDGEMENT

The authors would like to thank Karabük University Coordinatorship of Scientific Research Projects for the financial support with project number KBÜBAP-18-DR-005 and also Prof. Dr. Patricia Verleysen in the Material Laboratory of Ghent University.

REFERENCES

1. Kim, D. K., Kim, D. Y., Ryu, S. H., and Kim, D. J., "Application of nimonic 80A to the hot forging of an exhaust valve head", ***Journal Of Materials Processing Technology***, 113 (1–3): 148–152 (2001).
2. Zhu, Y., Zhimin, Y., and Jiangpin, X., "Microstructural

mapping in closed die forging process of superalloy Nimonic 80a valve head", ***Journal Of Alloys And Compounds***, 509 (20): 6106–6112 (2011).

3. Quan, G., Pan, J., and Wang, X., "Prediction of the Hot Compressive Deformation Behavior for Superalloy Nimonic 80A by BP-ANN Model", ***Applied Sciences***, 6 (3): 66 (2016).
4. Günay, M., Korkmaz, M. E., and Yaşar, N., "Finite element modeling of tool stresses on ceramic tools in hard turning", ***Mechanika***, 23 (3) (3): 432–440 (2017).
5. Korkmaz, M. E. and Günay, M., "Finite Element Modelling of Cutting Forces and Power Consumption in Turning of AISI 420 Martensitic Stainless Steel", ***Arabian Journal For Science And Engineering***, 43 (9): 4863–4870 (2018).
6. Gok, K., "Development of three-dimensional finite element model to calculate the turning processing parameters in turning operations", ***Measurement***, 75: 57–68 (2015).
7. Parida, A. K. and Maity, K., "Numerical and experimental analysis of specific cutting energy in hot turning of Inconel 718", ***Measurement***, 133: 361–369 (2019).
8. Jain, A., Khanna, N., and Bajpai, V., "FE simulation of machining of Ti-54M titanium alloy for industry relevant outcomes", ***Measurement***, 129: 268–276 (2018).
9. Parida, A. K. and Maity, K., "Effect of nose radius on forces, and process parameters in hot machining of Inconel 718 using finite element analysis", ***Engineering Science And Technology, An International Journal***, 20 (2): 687–693 (2017).
10. Asif. M, M., Shrikrishana, K. A., and Sathiya, P., "Finite element modelling and characterization of friction welding on UNS S31803 duplex stainless steel joints", ***Engineering Science And Technology, An International Journal***, 18 (4): 704–712 (2015).
11. Parida, A. K. and Maity, K., "Comparison the machinability of Inconel 718, Inconel 625 and Monel 400 in hot turning operation", ***Engineering Science And Technology, An International Journal***, 21 (3): 364–370 (2018).
12. Şerban, D. A., Marsavina, L., Rusu, L., and Negru, R., "Numerical study of the behavior of magnesium alloy AM50 in tensile and torsional loadings", ***Archive Of Applied Mechanics***, (1): 1–7 (2018).
13. Dorogoy, A. and Rittel, D., "Determination of the johnson-cook material parameters using the SCS specimen", ***Experimental Mechanics***, 49 (6): 881–885 (2009).
14. Schindler, S., Steinmann, P., Aurich, J. C., and Zimmermann, M., "A thermo-viscoplastic constitutive law for isotropic hardening of metals", ***Archive Of Applied Mechanics***, 87 (1): 129–157 (2017).
15. Yin, T., Bai, L., Li, X., Li, X., and Zhang, S., "Effect of thermal treatment on the mode I fracture toughness of granite under dynamic and static coupling load", ***Engineering Fracture Mechanics***, 199: 143–158 (2018).
16. Verleysen, P. and Degrieck, J., "Experimental investigation of the deformation of Hopkinson bar specimens", ***International Journal Of Impact Engineering***, 30 (3): 239–253 (2004).
17. Lee, S., Kim, K.-M., Park, J., and Cho, J.-Y., "Pure rate effect on the concrete compressive strength in the split Hopkinson pressure bar test", ***International Journal Of Impact Engineering***, 113: 191–202 (2018).
18. Nguyen, K.-H., Kim, H. C., Shin, H., Yoo, Y.-H., and Kim, J.-B., "Numerical investigation into the stress wave transmitting characteristics of threads in the split Hopkinson tensile bar test", ***International Journal Of Impact Engineering***, 109: 253–263 (2017).
19. Karkalos, N. E. and Markopoulos, A. P., "Determination of Johnson-Cook material model parameters by an optimization approach using the fireworks algorithm", ***Procedia Manufacturing***, 22: 107–113 (2018).
20. Tan, Y. B., Ma, Y. H., and Zhao, F., "Hot deformation behavior and constitutive modeling of fine grained Inconel 718 superalloy", ***Journal Of Alloys And Compounds***, 741: 85–96 (2018).
21. Limbadri, K., Toshniwal, K., Suresh, K., Kumar Gupta, A., V Kutumbarao, V., Ram, M., Ravindran, M., and Kalyankrishnan, G., "Stress Variation of Zircaloy-4 and Johnson Cook Model for rolled sheets.", ***Materials Today: Proceedings***, 5 (2): 3793–3801 (2018).
22. Ducobu, F., Rivière-Lorphèvre, E., and Filippi, E., "On the importance of the choice of the parameters of the Johnson-Cook constitutive model and their influence on the results of a Ti6Al4V orthogonal cutting model", ***International Journal Of Mechanical Sciences***, 122: 143–155 (2017).
23. Korkmaz, M. E., Verleysen, P., and Günay, M., "Identification of Constitutive Model Parameters for Nimonic 80A Superalloy", ***Transactions Of The Indian Institute Of Metals***, 71 (12): 2945–2952 (2018).
24. Samantaray, D., Mandal, S., and Bhaduri, A. K., "A comparative study on Johnson Cook, modified Zerilli-Armstrong and Arrhenius-type constitutive models to predict elevated temperature flow behaviour in modified 9Cr-1Mo steel", ***Computational Materials Science***, 47 (2): 568–576 (2009).
25. Calvo, J., Cabrera, J. M., Guerrero-Mata, M. P., De La Garza, M., and Puigjaner, J. F., "Characterization of the hot deformation behaviour of nimonic 80A and 263 Ni-based superalloys", ***Proceedings Of The 10th International Conference On Technology Of Plasticity, ICTP 2011***, Aachen, 892–896 (2011).
26. Sjöberg, T., Kajberg, J., and Oldenburg, M., "Fracture behaviour of Alloy 718 at high strain rates, elevated temperatures, and various stress triaxialities", ***Engineering Fracture Mechanics***, 178: 231–242 (2017).
27. ANSYS Workbench 19.1 Edition.
28. Korkmaz, M.E., "Determination and Verification of Johnson–Cook Parameters for 430 Ferritic Steels via Different Gage Lengths", ***Transactions of the Indian Institute of Metals,*** doi.org/10.1007/s12666-019-01734-9.
29. Korkmaz, M. E., Günay, M. and Verleysen, P., Investigation of tensile Johnson-Cook model parameters for Nimonic 80A superalloy, ***Journal of Alloys and Compounds***, 801: 542-549 (2019).